Biology of Reproduction, 2017, 96(1), 145–158
doi:10.1095/biolreprod.116.142752
Research Article
Advance Access Publication Date: 23 December 2016

Research Article

Natural killer-cell deficiency alters placental development in rats†

Stephen J. Renaud[1,2,*], Regan L. Scott[1,2], Damayanti Chakraborty[1,2], Mohammad A. K. Rumi[1,2] and Michael J. Soares[1,2,3,*]

[1]Institute for Reproductive Health and Regenerative Medicine, University of Kansas Medical Center, Kansas City, Kansas, USA; [2]Department of Pathology and Laboratory Medicine, University of Kansas Medical Center, Kansas City, Kansas, USA and [3]Department of Obstetrics and Gynecology, University of Kansas Medical Center, Kansas City, Kansas, USA

*Correspondence: Department of Anatomy and Cell Biology, Medical Sciences Building Rm 428, The University of Western Ontario, London, ON N6A 5C1, Canada. Tel: +1 519 661-2111 ×88272; Email: srenaud4@uwo.ca; or Institute of Reproductive Health and Regenerative Medicine, Department of Pathology and Laboratory Medicine, University of Kansas Medical Center, MS3050, 3901 Rainbow Boulevard, Kansas City, KS 66160, USA. Tel: +1-913-588-5691; Email: msoares@kumc.edu

†**Grant support:** This research was supported by NIH Grants HD020676 and HD082535.
Conference presentation: This research was partially presented at the Annual Meeting for the Society for the Study of Reproduction, Grand Rapids, MI (2014); and at Experimental Biology, San Diego, CA (2016).
Present address: Stephen J. Renaud, Department of Anatomy and Cell Biology, The University of Western Ontario, London, ON N6A 5C1, Canada.

Received 15 June 2016; Revised 2 December 2016; Accepted 6 December 2016

Abstract

Natural killer (NK) cells are the most prevalent leukocyte population in the uterus during early pregnancy. Natural killer cells contribute to uterine vascular (spiral artery) remodeling in preparation for the increased demand on these vessels later in pregnancy. A second wave of spiral artery modification is directed by invasive trophoblast cells. The significance of the initial wave of NK-cell-mediated vascular remodeling in species exhibiting deep trophoblast invasion such as humans and rats is not known. The purpose of this study was to generate a genetic model of NK-cell deficiency in rats, and determine the consequences of NK-cell deficiency on spiral artery remodeling and reproductive outcomes. To accomplish this task, we utilized zinc finger nuclease-mediated genome editing of the rat interleukin-15 (*Il15*) gene. *Il15* encodes a cytokine required for NK-cell lineage development. Using this strategy, a founder rat was generated containing a frameshift deletion in *Il15*. Uteri of females harboring a homozygous mutation at the *Il15* locus contained no detectable NK cells. NK-cell deficiency did not impact fetal growth or viability. However, NK-cell deficiency caused major structural changes to the placenta, including expansion of the junctional zone and robust, early-onset activation of invasive trophoblast-guided spiral artery remodeling. In summary, we successfully generated an NK-cell-deficient rat and showed, using this model, that NK cells dampen the extent of trophoblast invasion and delay trophoblast-directed spiral artery remodeling. This study furthers our understanding of the role of NK cells on uterine vascular remodeling, trophoblast invasion, and placental development.

Summary Sentence

Natural killer cells delay trophoblast invasion and trophoblast-directed spiral artery remodeling in rats.

Key words: natural killer cells, placenta, trophoblast, interleukin 15, invasion, spiral artery, vascular remodeling, pregnancy.

Introduction

A key event for successful pregnancy is the redirection of maternal blood to the placenta. One of the ways in which this task is accomplished is through remodeling the uterine spiral arteries—the vessels that supply the placenta with maternal blood—from low-flow vessels into high capacity conduits. Remodeling entails destabilization and removal of the smooth muscle and elastic laminae surrounding the spiral arteries [1]. Consequently, the vessels lose their tonic contraction and responsiveness to vasoactive compounds, resulting in a significantly increased internal luminal diameter. Remodeled spiral arteries are capable of carrying an enhanced and consistent supply of maternal blood to the placenta, thereby ensuring that the fetus obtains sufficient nutrients and gases to sustain growth and development. Two specialized cell types are thought to contribute to spiral artery remodeling: invasive trophoblast cells emanating from the placenta and maternal immune cells belonging to the natural killer (NK)-cell lineage [2].

Trophoblast cells comprise the epithelial component of the placenta. They differentiate into one of several distinct trophoblast lineages that have specialized functions depending on the anatomical compartment of the placenta in which they develop. Trophoblast cells adjacent to the decidua develop invasive properties [3]. These "invasive" trophoblast cells dissociate from the placenta and infiltrate the decidua, where they aggregate around and within the spiral arteries causing displacement of the native endothelium, and destruction of the surrounding elastic lamina and smooth muscle coat surrounding the vessels [1, 4]. Consequently, the spiral arteries become flaccid, distended, trophoblast-lined vessels that carry a large and unimpeded supply of maternal blood to the placenta. Trophoblast-directed spiral artery remodeling precedes the onset of robust fetal growth, and is a characteristic of hemochorial placentation—a type of placentation that occurs in humans, rats, mice, and many other species in which trophoblast cells directly contact maternal blood [5]. However, there is variability in the extent of trophoblast invasion between different species possessing this type of placentation. In mice, trophoblast invasion is shallow, and the extent of trophoblast-mediated spiral artery transformation is limited [6]. In comparison, trophoblast cells advance deep into the uterus in rats and humans, extending into the proximal third of the myometrium in humans and through the entire depth of the mesometrial compartment in rats [6, 7]. Defective trophoblast-directed spiral artery remodeling is a feature common to several obstetric complications (preeclampsia, intrauterine growth restriction, preterm birth, and late spontaneous abortion), underscoring the importance of this process in humans [8].

Prior to the onset of trophoblast infiltration, a contingent of NK cells accumulates within the decidua where they comprise approximately 70% of all leukocytes in the uterus during early pregnancy [9]. The accumulation of NK cells within the uterus contrasts with other lymphocytes, which are generally excluded from the implantation site. These uterine/decidual NK cells (referred to as uterine NK cells for the remainder of this manuscript) are phenotypically and functionally distinct from the majority of NK cells that reside within other tissues, in that they produce many cytokines and possess limited cytotoxic activities. The number of uterine NK cells dwindles around the time that trophoblast cells begin to invade into the uterus, and they are scarce by term [6, 10]. A clear picture of the function of uterine NK cells has yet to be elucidated. The prevailing stance is that these cells help to build a healthy placenta [11]. Pregnant mice genetically devoid of NK cells exhibit spiral arteries with narrow lumens, intact tunica media, and swollen endothelial cells, implying that NK cells are vital, either directly or indirectly, for guaranteeing correct spiral artery remodeling in this species [12]. In line with the importance of NK cells for facilitating placental blood flow, compromised fetal growth has been observed in mice lacking NK cells and in mice with reduced NK-cell function [13–15]. Natural killer cells appear to initiate angiogenesis and at least a partial "first wave" of spiral artery remodeling in humans and rats as well, since dilation and medial disorganization of spiral arteries is evident prior to the arrival of invasive trophoblast cells [16, 17]. The functional importance of this NK-cell-mediated initial phase of spiral artery modification in species that also demonstrate robust trophoblast-directed vascular remodeling is not clear.

To gain insight into the importance of NK cells in a species that also exhibits deep trophoblast invasion, we previously used an immunodepletion strategy to diminish NK cells in rats [16]. Consistent with a role for NK cells in the initial stages of spiral artery development, we found that NK-cell immunodepletion caused reduced oxygen delivery to the placenta early in pregnancy. Reduced oxygen delivery, in turn, resulted in accelerated trophoblast invasion and robust trophoblast-directed spiral artery remodeling. However, due to the transient nature of antibody-mediated immunodepletion, we were not able to determine the impact of NK-cell deficiency on placental and fetal development later in pregnancy. Thus, in this study, we used an alternative, genetic approach to generate rats devoid of NK cells: targeted genome editing of the *Interleukin-15* (*Il15*) locus via zinc finger nucleases. *Il15* was targeted because it encodes a cytokine that is critical for NK-cell survival and maturation [18]. Thus, NK cells should not be detected in rats lacking *Il15*. In this study, we characterize the *Il15*-deficient rat model, determine the impact of *Il15* deficiency on uterine NK-cell development, and describe alterations in placental development and reproductive outcomes in these rats.

Materials and methods

Animals

Holtzman Sprague-Dawley rats were purchased from Harlan Sprague-Dawley. Rats were maintained in a 14 h light:10 h dark cycle (lights on at 0600 h) with food and water available ad libitum. The University of Kansas Medical Center Animal Care and Use Committee approved all protocols involving the use of rats.

Generation and identification of targeted *Il15* mutation

Zinc finger nucleases are bioengineered fusion proteins containing (i) zinc finger proteins conferring nucleotide sequence-specific

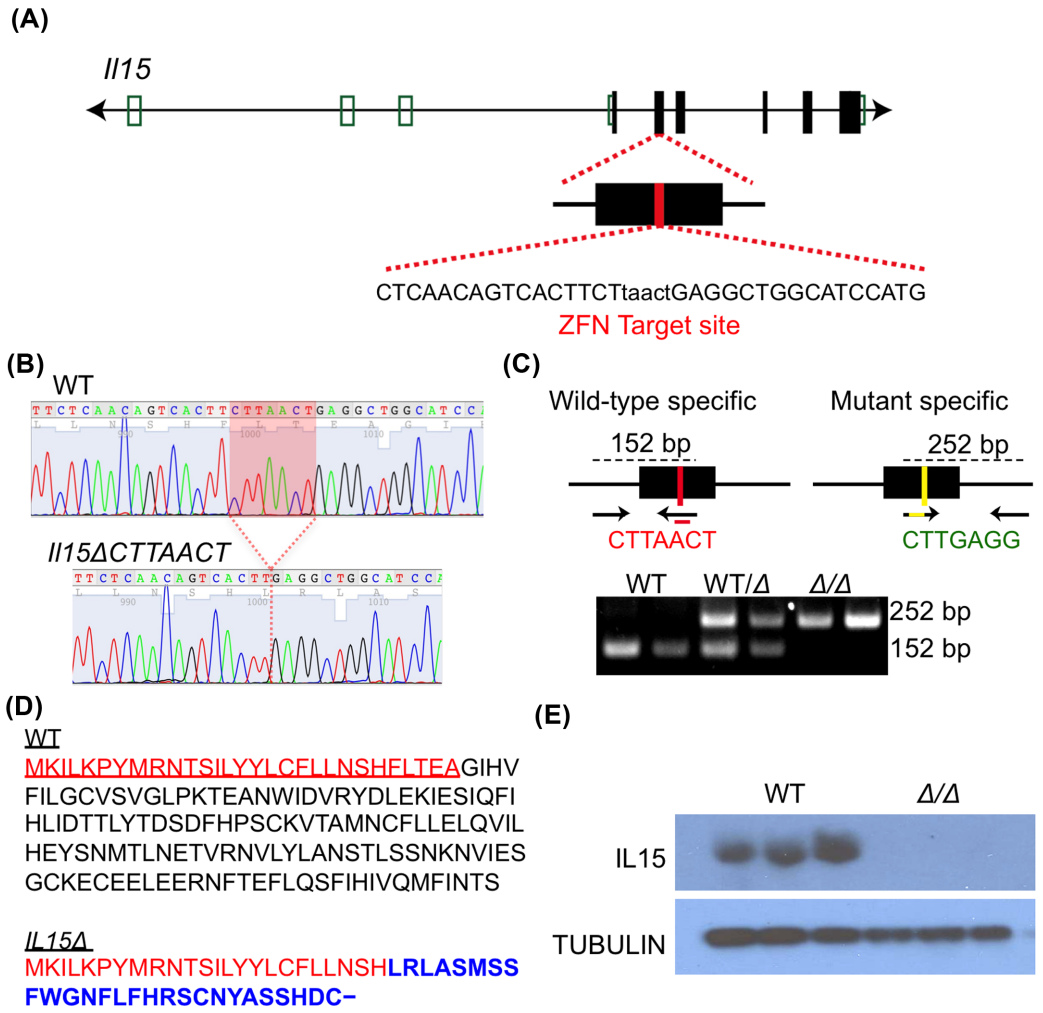

Figure 1. Zinc finger nuclease (ZFN)-mediated genome editing of the rat *Il15* locus. (**A**) ZFN target site recognizing a sequence within the second coding exon of rat *Il15*. (**B**) Sequencing results of genomic DNA extracted from a wild-type (WT) pup and a founder pup containing a 7-bp deletion (*Il15*ΔCTTAACT—referred to *Il15*Δ in the remainder of the figure) within the second coding exon of *Il15*. (**C**) Genotyping strategy used to identify rats containing the wild-type *Il15* allele and/or the *Il15*Δ allele. The upper, 366-bp band common to all genotypes has been omitted. (**D**) Predicted amino acid sequences encoded by WT-*Il15* and *Il15*Δ. Letters in red indicate the sequence of the leader peptide. Letters in blue are deviations from the WT sequence. (**E**) Western blot showing IL15 protein in rat spleen tissue. Tubulin was used as a loading control.

DNA binding and (ii) *FokI* endonuclease that creates double-strand DNA breaks at the target locus. Imperfect repair of double-strand DNA breaks induced by site-specific endonuclease activity results in mutations at high efficiencies, including frameshift deletions that result in functional gene knockouts [19]. Zinc finger nuclease constructs specific for the rat *Il15* locus were designed and validated by Sigma Aldrich (St. Louis, MO). A construct targeting the second exon of *Il15* was selected. The target sequence was CTCAACAGTCACTTCTtaactGAGGCTGGCATCCATG, which corresponds to nucleotides 61–97 in rat *Il15* mRNA (NM_013129.2, Figure 1A). Single cell rat embryos were collected from the oviducts of embryonic day (E)0.5 rats. Transcripts encoding the selected zinc finger nucleases were microinjected into embryos. Embryos were then transferred into oviducts of pseudopregnant E0.5 rats. Offspring were initially screened for mutations via isolating genomic DNA from tail-tip biopsies using the E.Z.N.A. tissue DNA kit (Omega Bio-Tek, Norcross, GA). Polymerase chain reaction (PCR) was performed on the purified DNA samples using primers flanking the zinc finger nuclease site, and products resolved by agarose gel electrophoresis and ethidium bromide staining. Genomic DNA containing potential mutations was amplified by PCR, gel purified, and subcloned into TOPO-TA vectors (Thermo Fisher Scientific, Waltham, MA). Vectors were then transformed into XL-10 Gold ultracompetent *Escherichia coli* (Agilent Technologies, Santa Clara, CA), plated onto LB-agar plates containing 20 mM isopropyl β-D-1-thiogalactopyranoside, 80 μg/ml 5-bromo-4-chloro-3-indolyl-β-D-galactopyranoside, and 100 μg/ml ampicillin, and 20 colonies were selected for sequencing (Genewiz Inc, South Plainfield, NJ). A founder rat possessing a frameshift deletion in *Il15* was identified and backcrossed to wild-type rats to show germline transmission. For all experiments, *Il15* heterozygotes were intercrossed to produce wild-type, heterozygote, and homozygous mutant offspring. Offspring were grown to adulthood, and experiments were performed on pregnant female wild-type and homozygous mutant offspring. Pregnancy was achieved by breeding wild-type and homozygous mutant offspring with

Table 1. List of primers used for genotyping and sexing.

Primer name	Sequence
Il15 F1552	ACAATGCAGTCTTCCTGTTTTT
Il15 F1666	CTTCTCAACAGTCACTTGAGGC
Il15 R1918	ACTGCCAAGGTGCTGAAATC
Il15 R1704*	ATGGATGCCAGCCTCAGTTA
Kdm5c/Kdm5d	GAAGCCTTTGGCTTTGAGC
Kdm5c/Kdm5d	CCGCTGCCAAATTCTTTGG

*Il15 R1704 is complementary to a sequence only present in the mutant allele.

wild-type males. The *Il15* mutant rat model is available at the Rat Resource & Research Center (University of Missouri; RRRC#769; http://www.rrrc.us/).

Genotyping

Genotyping was performed using DNA extracted from tail-tip biopsies. DNA was purified with the RedExtract-N-Amp tissue PCR kit (Sigma-Aldrich) using directions provided by the manufacturer. Four primers were used to distinguish between wild-type and mutant *Il15* loci. The sequences of these primers are provided in Table 1. One forward and one reverse primer produced a 366-bp band that was common to both wild-type and mutant loci. A second forward primer spanned a sequence only present in the mutant allele (i.e., overlapping the zinc finger nuclease cut site). This second forward primer and the common reverse primer produced a 252-bp band that identified the mutant locus. A second reverse primer included a sequence that was present only in the wild-type allele (i.e., including the zinc finger nuclease target site that was deleted in mutant alleles). This second reverse primer and the common forward primer produced a 152-bp band that identified the wild-type allele. Hence, wild-type rats were identified by a 366-bp band and a 152-bp band; homozygous mutant rats were identified following detection of a 366-bp band and a 252-bp band. All three bands were detectable in heterozygous samples.

Flow cytometry

Blood was collected from 7-week-old male rats, layered over Lymphoprep (StemCell Technologies, Vancouver,BC, Canada), and subjected to density-gradient centrifugation to enrich lymphocytes according to the manufacturer's instructions. Spleen tissue was harvested and mechanically dissociated to extract splenocytes. Splenocytes were passed through a 100-μm cell strainer and incubated with ACK lysis buffer (Thermo Fisher Scientific) to remove erythrocytes. Subsequently, 1×10^6 cells from blood or spleen were incubated for 30 min with 10% normal goat serum and 5 μg/ml rat IgG (both from Thermo Fisher Scientific) to block nonspecific antibody binding sites, then incubated for 40 min with phycoerythrin-conjugated mouse anti-rat anti-KLRB1A (BD Pharmingen 550270), alexa 488-conjugated mouse anti-rat CD68 (Biorad MCA341A488), allophycocyanin-conjugated mouse anti-rat CD3 (BD Pharmingen 557030), or unconjugated mouse anti-rat CD32 (BD Pharmingen 550270). All cells were washed in PBS containing 2% fetal bovine serum, and then CD32-labeled cells were incubated for 30 min with a pacific blue-conjugated goat anti-mouse antibody followed by an additional wash. Cells were then analyzed using a BD LSRII flow cytometer.

Assessment of fetal growth and maternal organ weight

The stage of the estrous cycle was determined by the assessment of cell populations within vaginal lavages. On proestrus, wild-type and *Il15* mutant rats were co-habited with a fertile, wild-type male, and the presence of sperm the following morning was designated E0.5. Rats were euthanized by CO_2 asphyxiation on E13.5, E18.5, and E19.5. Whole placentation sites were removed and either placed into dry ice-cooled heptane for subsequent immunohistochemical analysis or further dissected. In dissected placentation sites, fetuses were removed, assessed for viability and morphological defects, weighed, and sex determined (at E18.5 only). Sex was determined by PCR on genomic DNA for *Kdm5c* (X chromosome) and *Kdm5d* (Y chromosome), using primers detailed in Table 1, based on a modification of a previously described procedure [20]. Uterine tissue adjacent to developing placentation sites (decidua and mesometrial triangle) was removed and frozen in liquid nitrogen for molecular analyses. Maternal spleen was also wholly excised, weighed, and frozen in liquid nitrogen.

Western blotting

Expression of IL15 was determined in splenic tissue by western blotting. Splenic lysates were prepared in buffer containing 62.5 mM Tris (pH 6.8), 10% glycerol, 2% sodium dodecyl sulfate (SDS), and 50 mM dithiothreitol. Approximately 10 μg protein was electrophoretically separated in SDS-PAGE gels and transferred to polyvinylidene fluoride membranes. Membranes were subsequently blocked with 5% milk, and probed using an antibody specific for IL15 (sc-7889, 0.2 μg/ml, Santa Cruz Biotechnology, Santa Cruz, CA). An antibody detecting alpha-tubulin (0.05 μg/ml, clone CP06, EMD-Millipore Corp, Billerica, MA) was used as a loading control. Membranes were then incubated with species appropriate horseradish peroxidase-conjugated antibodies, immersed in Luminata Classico enhanced chemiluminescence reagent (EMD-Millipore Corp), and luminescence detected using GeneMate basic blue autoradiography film (Bioexpress, Kaysville, CT).

RT-PCR

RNA was extracted by homogenizing tissue in Tri-Reagent (Sigma-Aldrich), according to a protocol provided by the manufacturer. Purified RNA (500 ng) was used for reverse transcription using the High Capacity cDNA Reverse Transcription kit (Applied Biosystems, Foster City, CA). Complementary DNAs were diluted 1:10, and subjected to quantitative RT-PCR (qRT-PCR) using SYBR Green PCR Master Mix (Thermo Fisher Scientific) and primers described in Table 2. An ABI Prism 7500 Real Time PCR system (Thermo Fisher Scientific) was used for amplification and fluorescence detection. Cycling conditions were as follows: an initial holding step (95°C, 10 min), followed by 40 cycles of two-step PCR (95°C for 15 s, 60 C for 1 min), and then a dissociation step (95°C for 15s, 60°C for 15 s, and a sequential increase to 95°C). Relative mRNA expression was calculated using the $\Delta\Delta$Ct method. *Rn18s* was used as a reference RNA.

Histology and immunohistochemistry

Frozen placentation sites were embedded in OCT compound and cryosectioned at 8 μm thickness, fixed in 4% paraformaldehyde, and either stained with hematoxylin and eosin or incubated overnight with antibodies recognizing perforin (5 μg/ml, Torrey Pines Biolabs, Secaucus, NJ), vimentin (V6389, 5 μg/ml Sigma-Aldrich), and alpha smooth muscle actin (5 μg/ml, clone 1A4, Sigma-Aldrich). Sections

Table 2. List of primers used for RT-PCR.

Gene	Accession no.	Forward primer	Reverse primer	Size (bp)
Prf1	NM_017330.2	GGCACTCAAGAACCTTCC	CTCAAGCAGTCTCCTACC	192
Ifng	NM_138880.2	ACAACCCACAGATCCAGCAC	GACTCCTTTTCCGCTTCCTT	95
Ncr1	NM_057199.1	ATGGGAACATCCAAGCAGAG	ACAGGCTCACTGGGAAAAGA	114
Ly49s5/i5	NM_001012749.1/ NM_001009501.2	TTTTAGCTTCCCCTCAGCAC	TGTAGTTCTGGCAGGTCTGTTT	129
Ly49s3/s4/i3/i4	NM_153726.1/ NM_001009487.1/ NM_001009499.1/ NM_001009495.1	TTAGCTTCCCCTCAGCACAC	TGTTTACATTCACGCCATATTCTT	109
Klrb1a	NM_001010964.1	CGTTCACACAGGTTGGCTTT	TGGCTCCACTGATGGTTTTT	116
Klrb1c	NM_001085403.1	GTCTCCAGGGCATAAGCAAG	AAGAAGGATCAGCGTAGCACA	111
Klrb1	NM_001085405.1	GGTCTCGCTGACTGTTCTTTG	TTGTTGTCCTTTTCCCTTTG	101
Lamp1	NM_012857.2	ACAGGTTTGGGTCTGTGGAA	GATGAGGTAGGCGATGAGGA	99
Il18	NM_019165.1	ATGCCTGATATCGACCGAAC	TAGGGTCACAGCCAGTCCTC	95
Rn18s	NR_046237.1	GCAATTATTCCCCATGAACG	GGCCTCACTAAACCATCCAA	123

were then immersed in species-appropriate fluorescent-conjugated secondary antibodies. A fluorescein isothiocyanate-conjugated pan-cytokeratin antibody (1:50 dilution, F3418, clone C-11, Sigma-Aldrich) was used to identify trophoblast cells. Sections were then incubated with 4′,6-diamidino-2-phenylindole (DAPI, Thermo Fisher Scientific) to identify nuclei, mounted with Fluoromount-G mounting media (SouthernBiotech, Birmingham, AL), and examined microscopically.

Statistical analysis

To estimate the size of the labyrinth and junctional zones, a line was drawn around the perimeter of each respective zone. Delineation of zones was facilitated using immunohistochemistry for vimentin. The resulting pixel area of each zone was tabulated using ImageJ software [21]. To assess the depth of trophoblast invasion, a line was drawn from the peripheral edge of the junctional zone to the distal-most spiral artery containing endovascular trophoblast cells. The length of this line was calculated using ImageJ software. When sectioning, detection of the central maternal arterial channel was used as a landmark to indicate the center of the placenta. In all experiments, statistical comparisons between two means were performed using the Student *t*-test. Comparisons of multiple groups were evaluated using analysis of variance. The source of variation from significant *F*-ratios was determined using the Tukey multiple comparison test. Results were deemed statistically significant when $P < 0.05$. All experiments were conducted at least in triplicate. Graphing and statistical analysis was conducted using GraphPad Prism 6.0 (GraphPad Software Inc., La Jolla, CA).

Results

Identification of a mutation within the rat *Il15* locus induced by zinc finger nucleases

Zinc finger nucleases targeting *Il15* were microinjected into rat embryos. Following transfer of embryos to a recipient rat, a male pup was identified containing a 7-bp (*Il15*ΔCTTAACT, Figure 1B) monoalleleic frameshift deletion within exon 2 of the rat *Il15* gene. The mutant locus is referred to as *Il15*Δ for the remainder of the manuscript. The founder male rat was mated with female wild-type rats, and half the progeny possessed one wild-type and one mutant allele, thus demonstrating germline transmission of the mutation.

Table 3. Genotype of offspring following heterozygous breeding.

	n	%
WT	71	30.0
WT/Δ	107	45.1
Δ/Δ	59	24.9

An example of the PCR-based strategy used to genotype rats is provided in Figure 1C. The frameshift resulted in an alteration in the predicted amino acid sequence, leading to a premature stop codon (Figure 1D). Consistent with the frameshift mutation, mature IL15 protein was not detected in mutant homozygotes as determined by western blotting (Figure 1E). Mating of heterozygotes produced the expected Mendelian complement of wild-type, heterozygote, and homozygous mutant *Il15* rats (Table 3), and the anticipated frequency of male and female offspring.

Effect of *il15* deficiency on immune cell populations in blood, spleen, and uterus

Il15 encodes a cytokine that is implicated in the growth, development, and survival of specific immune cell subtypes, so we next examined whether differences in populations of select immune cell lineages are apparent between wild-type and *Il15*Δ/Δ rats. The percentage of lymphocyte-enriched blood cells and splenocytes possessing CD3, a coreceptor expressed by T cells, or CD32 (also known as FcγRII), a protein expressed predominantly on the surface of B cells, was unchanged between wild-type and *Il15*Δ/Δ rats (Figure 2). CD68 (monocytes/macrophages) was not readily detected in blood due to our isolation protocol to enrich lymphocyte populations. In spleen, the percentage of cells expressing CD68 was not substantially altered between wild-type and *Il15*Δ/Δ rats (0.8% in wild-type rats, 1.0% in *Il15*Δ/Δ rats). In contrast, the percentage of cells possessing high surface expression of KLRB1A (also called NKR-P1A or CD161A), a protein expressed predominantly on the surface of NK cells, was reduced by ∼93% (n = 3 rats, $P < 0.05$, Figure 2). The vast majority of these KLRB1A^{hi} cells (99% in blood, 97% in spleen) did not express CD3, confirming that the majority of these cells are not T cells (Supplementary Figure S1). The percentage of cells possessing low cell surface expression of KLRB1A was not significantly altered in either blood or spleen between wild-type and *Il15*Δ/Δ rats (Figure 2).

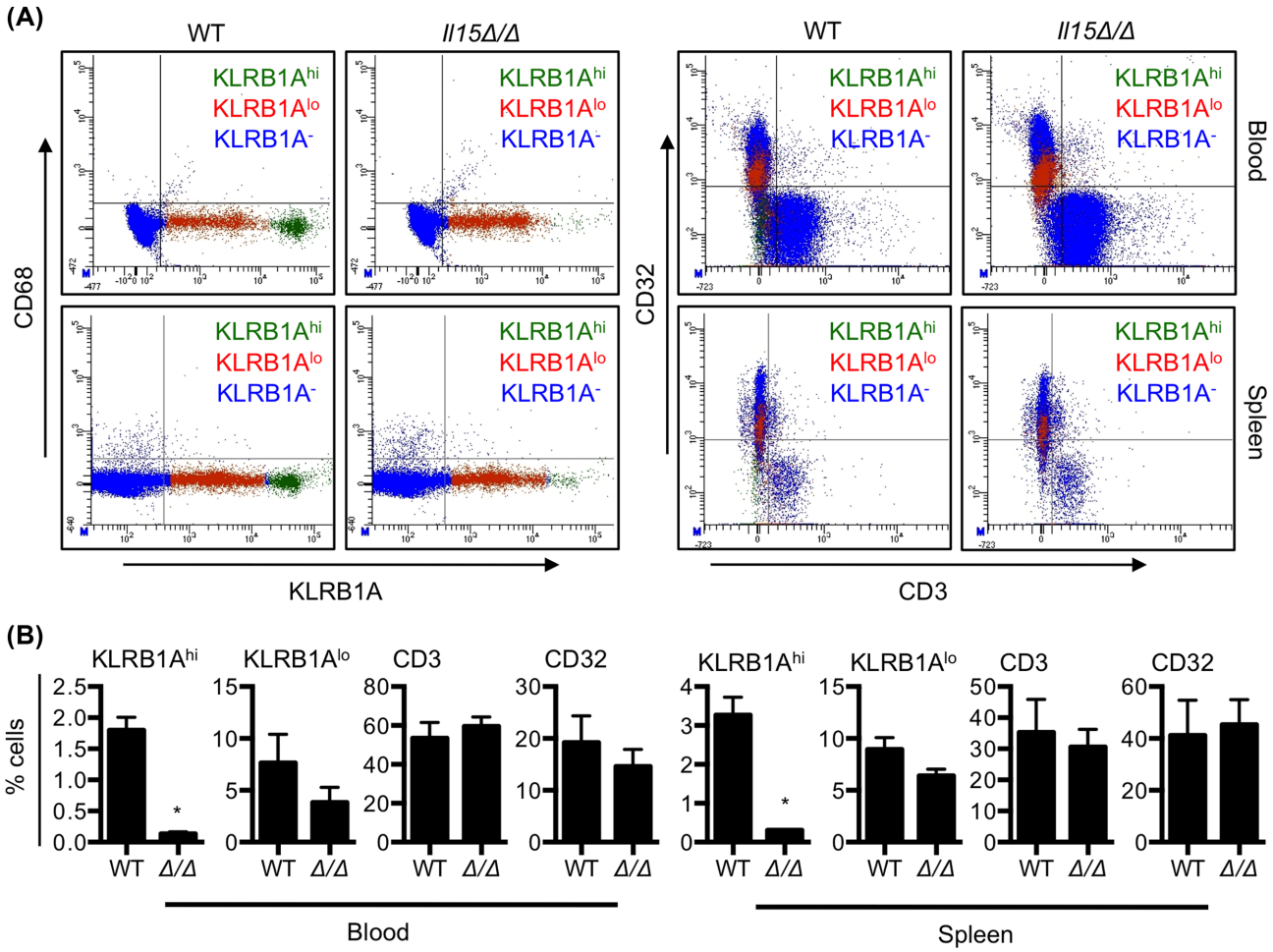

Figure 2. Reduced numbers of NK cells in *Il15*Δ/Δ rats. (**A**) Representative flow cytometric images for KLRB1A and CD68 (left panels) and for CD32 and CD3 (right panels) in lymphocyte-enriched blood cells and splenocytes collected from wild-type (WT) and *Il15*Δ/Δ rats. (**B**) Graphical representation of the percentage of KLRB1A^{hi}, KLRB1A^{lo}, CD3^{+}, and CD32^{+} cells in lymphocyte-enriched blood cells and splenocytes isolated from WT and *Il15*Δ/Δ rats. Graphs represent means +/− SEM. Asterisks denote statistical significance (*, $P < 0.05$, n = 3).

To additionally examine differences in NK-cell numbers between wild-type and *Il15*Δ/Δ rats, expression of perforin was assessed in spleen and uterus. Perforin is a pore-forming protein found in most subsets of NK cells and cytotoxic T lymphocytes. The pregnant uterus possesses an abundant population of NK cells whereas cytotoxic T lymphocytes are scarce [10], so detection of perforin within this tissue was used as a marker of NK cells. Perforin immunofluorescence was robust in wild-type rat spleen, and even more so in wild-type uteri on E13.5. In contrast, *Il15*Δ/Δ rats possessed very little evidence of perforin in spleen, and perforin was undetectable in E13.5 uteri (Figure 3A). To further assess NK cells in *Il15*Δ/Δ uteri, qRT-PCR analysis was performed on E13.5 uterine lysates. Compared to uterine lysates from wild-type rats, expression of a variety of genes associated with NK cells was nullified in uterine lysates prepared from *Il15*Δ/Δ uteri (Figure 3B). Transcripts that were included in our expression analysis included *Prf1 (*encodes perforin), *Ifng* (encodes interferon-gamma), and transcripts encoding a variety of receptors expressed specifically by NK cells, including *Ly49s5/i5* and *Ly49s3/s4/i3/i4* (which encode Ly49/killer cell lectin-like A receptors), *Klrb1*, *Klrb1a,* and *Klrb1b* (which encode killer cell lectin-like B receptors), and *Ncr1 (*natural cytotoxicity triggering receptor, also called NKp46). Expression of other transcripts was unaffected (*e.g. Il18* and *Lamp1*). Collectively, these data indicate that *Il15*Δ/Δ rats possess a deficiency in NK cells.

Il15 deficiency affects maternal body and spleen weight

IL15-deficient mice do not exhibit changes in body size or organ weight [22], but IL15 receptor alpha-deficient mice show smaller overall body size and reduced spleen weight compared to wild-type mice [23]. This prompted an investigation into changes in body and spleen weights between wild-type and *Il15*-deficient rats. Non-pregnant wild-type rats and their *Il15*Δ/Δ sisters did not differ in body weight, but *Il15*Δ/Δ rats exhibited a 25% reduction in absolute spleen weight (Figure 4, $P < 0.05$, n = 5). Consequently, the spleen:body weight ratio was reduced in *Il15*Δ/Δ rats. During pregnancy, a 46% increase in the size of the spleen was observed in wild-type rats compared to nonpregnant wild-type rats, which is consistent with what is reported elsewhere [24]. *Il15*Δ/Δ rats showed a comparable increase (69%) in the size of the spleen during pregnancy, indicating that IL15 deficiency did not impair splenic growth induced by pregnancy. However, in comparison to wild-type rats,

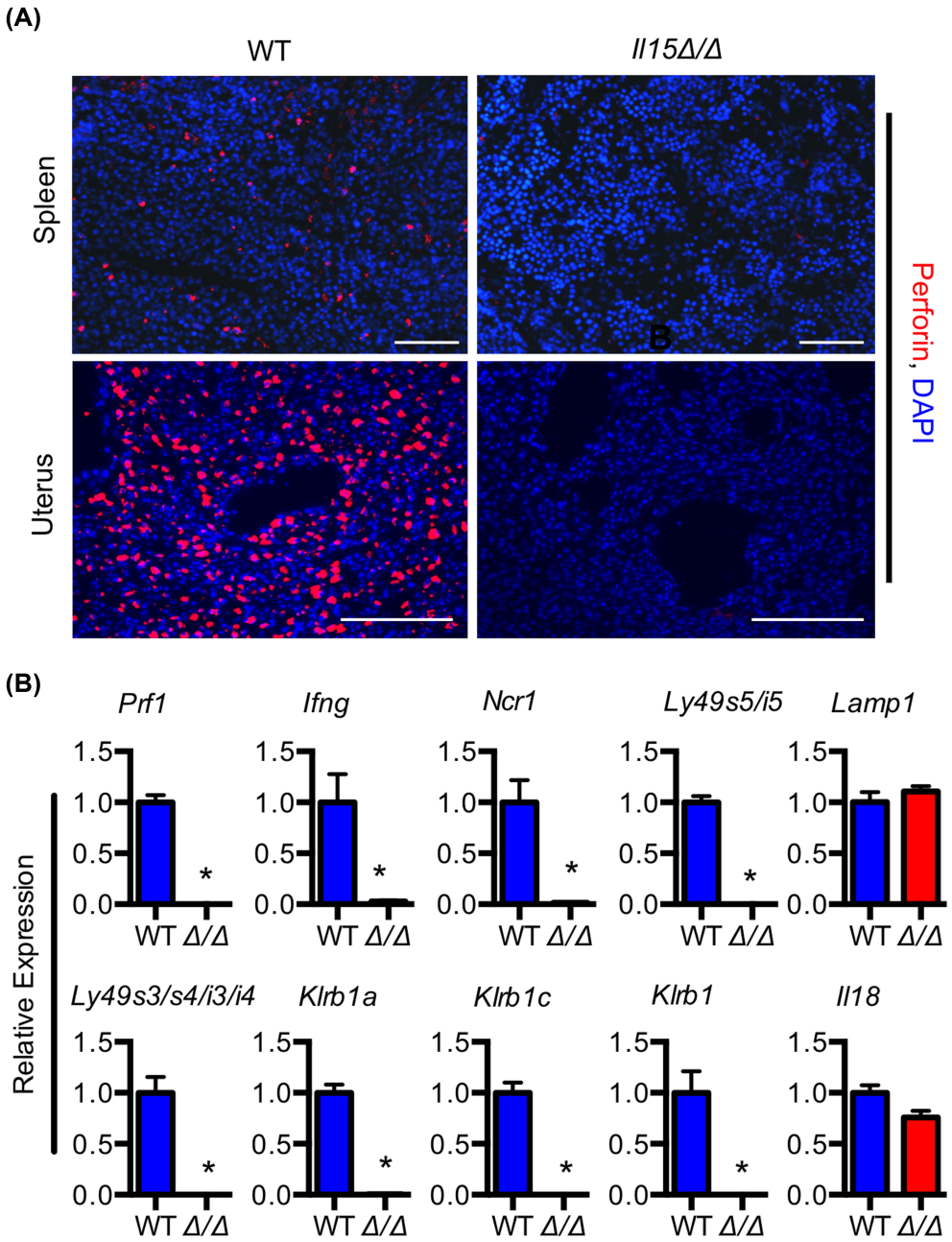

Figure 3. Natural killer cells are not detected in uterus of *Il15*Δ/Δ rats. (**A**) Perforin immunostaining in spleen and E13.5 uterine tissue in wild-type (WT) and *Il15*Δ/Δ rats. DAPI was used to identify nuclei. (**B**) Quantitative RT-PCR analysis of various transcripts in E13.5 uterine tissue collected from E13.5 WT and *Il15*Δ/Δ rats. Graphs represent means +/− SEM. Asterisks denote statistical significance (*, $P < 0.05$, n = 3). Scale bar = 100 μm.

*Il15*Δ/Δ rats exhibited a reduced absolute spleen weight (14% less, $P < 0.05$, n = 8) on E18.5, and also a slight reduction in overall body size (Figure 4, 6% less, $P < 0.05$).

Effect of *il15* deficiency on pregnancy outcome

Since uterine NK cells were undetectable in *Il15*-deficient rats, our next goal was to determine whether any differences in fetal and maternal health were evident in rats lacking uterine NK cells. Compared to wild-type rats, rats deficient in NK cells did not exhibit a significant difference in the percentage weight gain of dams during pregnancy ($P > 0.05$, n = 4 dams). There was also no significant difference in litter size or embryo viability between wild-type and *Il15*Δ/Δ rats ($P > 0.05$, n = 8 for WT, n = 9 for *Il15*Δ/Δ). Likewise, there was no difference in fetal weight between wild-type and *Il15*Δ/Δ dams at E13.5 ($P > 0.05$, n = 21 fetuses for wild-type, n = 23 fetuses for *Il15*Δ/Δ), and no significant difference in weight of fetuses (matched for sex) at E18.5 (Figure 5, n ≥ 30 fetuses for each group). There was also no evidence of gross fetal morphological defects, placental weight, or the expected date of parturition. Thus, pregnancy appeared to progress uneventfully in the absence of uterine NK cells.

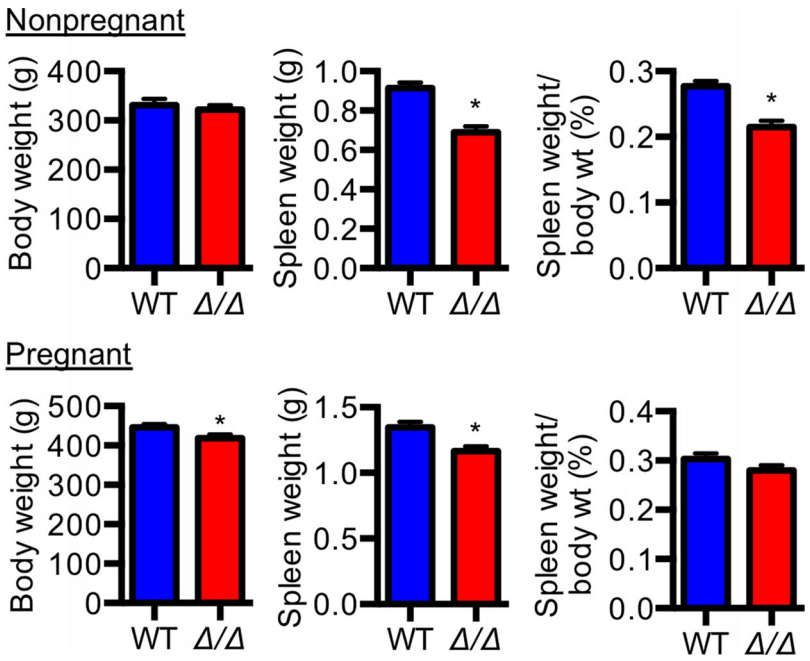

Figure 4. Effect of IL15 deficiency on body and spleen weight in nonpregnant and pregnant rats. Body weight, spleen weight, and spleen:body weight ratio in nonpregnant and E18.5 pregnant wild-type (WT) and *Il15*Δ/Δ rats. Graphs represent means +/− SEM. Asterisks denote statistical significance (*, $P < 0.05$, n = 5 for each nonpregnant group, and n = 8 for each pregnant group).

Placental adaptations in response to the absence of natural killer cells

Natural killer cells within the uterus have previously been implicated as key regulators of decidualization and placentation [11]. Thus, we next assessed the structure of placentation sites in wild-type and *Il15*Δ/Δ uteri using hematoxylin and eosin staining. In comparison to the mesometrial compartment of wild-type animals, eosinophilic staining was lacking around the spiral arteries of the mesometrial compartment of *Il15*Δ/Δ animals (Supplementary Figure S2), which we attribute to a lack of NK cells since this is where these cells would normally reside. However, we did not observe substantial deficits in decidual stromal organization or cellularity, which differed from what was reported in decidua of $Il15^{-/-}$ mice [13].

Our next goal was to determine the effect of NK-cell deficiency on placental development. The rodent placenta can be anatomically divided into two compartments: (i) the *labyrinth* zone, which is where exchange of nutrients, gases, and wastes between maternal and fetal blood takes place and (ii) the *junctional* zone, which forms the interface between placental and decidual tissue and is the site where invasive trophoblast cells develop [25]. Using vimentin immunostaining to distinguish compartments within the placentation site (uterine decidua, positive; junctional zone, negative; labyrinth zone, positive), we noted a 1.6-fold increase in the volume of the junctional zone in rats lacking NK cells (Figure 6, $P < 0.05$, n = 5). In contrast, there was no significant difference in the size of the labyrinth zone at either time point. Consequently, NK-cell-deficient rats had a significant increase in the junctional zone: labyrinth zone ratio compared to wild-type rats (Figure 6, $P < 0.05$, n = 5).

Effect of natural killer-cell deficiency on spiral artery remodeling

Since NK cells contribute to the initial stages of spiral artery transformation, our next goal was to determine whether NK-cell deficiency affected the degree of spiral artery transformation. On E13.5, rats lacking NK cells exhibited dilated spiral arteries with substantially increased internal luminal diameters compared to wild-type rats. Using cytokeratin immunostaining, it was apparent that the depth of trophoblast invasion was extensive in NK-cell-deficient rats, and that spiral arteries had already been infiltrated by invasive trophoblast cells (Figure 7A–C, n = 4). Moreover, trophoblast infiltration of the spiral arteries was associated with substantial loss of vascular smooth muscle cells relative to vessels lacking trophoblast cells (Figure 7D and E). In comparison, trophoblast invasion was modest or nonexistent at E13.5 in wild-type rats, and spiral arteries were encircled by a relatively continuous layer of vascular smooth muscle. By E19.5, the increase in the size of the junctional zone in NK-cell-deficient rats was still apparent. However, extensive trophoblast invasion and vascular remodeling were evident in both wild-type and NK-cell-deficient rats (Figure 8).

Discussion

The purpose of this study was to generate rats exhibiting a genetic deficiency in NK-cell lineage development, and determine the impact of maternal NK-cell deficiency on placental formation and fetal outcomes. To accomplish this task, the *Il15* locus was disrupted in early rat embryos using microinjection of zinc finger nucleases. IL15 was targeted because it encodes a cytokine that is critical for NK-cell viability, maturation, functional activity, and expansion [18]. IL15 is broadly expressed by many tissues, and signals through a heterotrimeric IL15 receptor, which is restricted to the surface of NK cells, subsets of T cells, and mitogen-activated macrophages [26]. Mice possessing a targeted disruption of the gene encoding IL15, IL15 receptor components, or signaling cascades that operate downstream of IL15 receptor activation are devoid of NK cells, and have severely reduced numbers of NK-T cells, memory CD8+

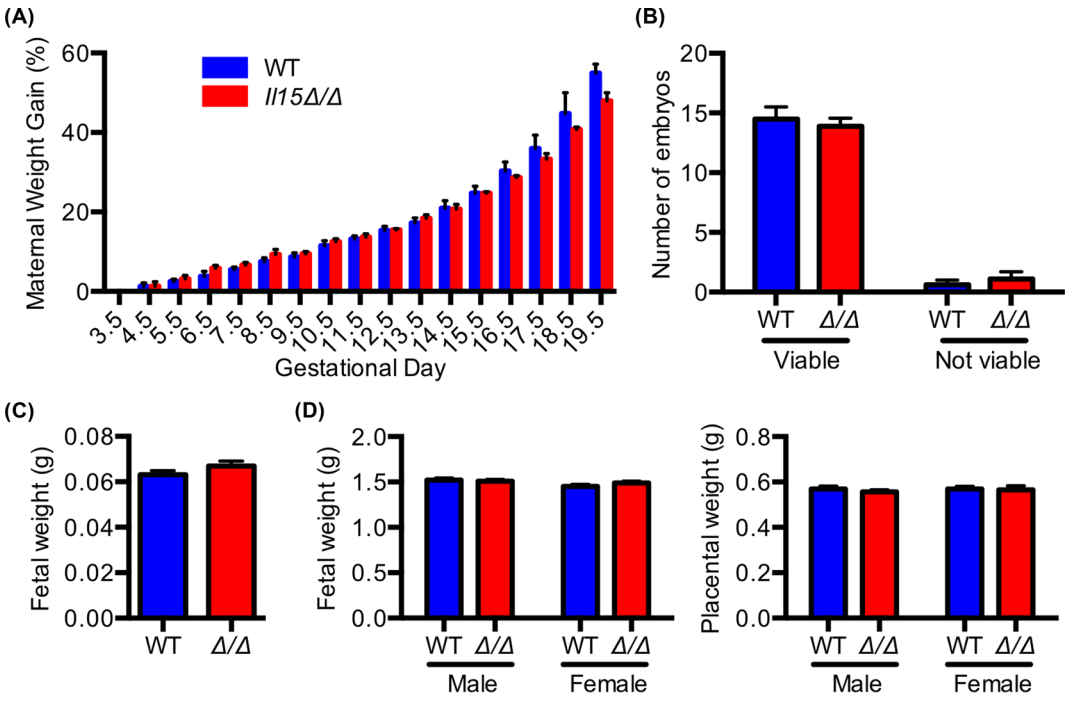

Figure 5. Effect of NK-cell deficiency on pregnancy outcome in rats. (**A**) Percentage weight gain throughout pregnancy in wild-type (WT) and *Il15*Δ/Δ dams (n = 4). (**B**) Total number of viable and nonviable embryos on E18.5 in WT and *Il15*Δ/Δ dams (n = 8 for WT, n = 9 for *Il15*Δ/Δ). (**C**) Fetal weight in WT and *Il15*Δ/Δ dams on E13.5 (n = 21 fetuses for WT, 23 fetuses for *Il15*Δ/Δ). (**D**) Sex-specific fetal and placental weights determined on E18.5 in WT and *Il15*Δ/Δ dams (n ≥ 30 fetuses per group). Graphs represent means +/− SEM.

T cells, and subsets of intraepithelial lymphocytes in the intestine [22, 27, 28]. Uterine NK-cell expansion in mice is also contingent on IL15 [13, 29]. In the current study using rats, we identified a similar dependency on IL15 for NK-cell development. Thus, by genetically disrupting the gene encoding IL15, we successfully abrogated uterine NK cells in rats. An important caveat to this study is that, although we did not detect differences in the total number of $CD3^+$ T cells, $CD32^+$ B cells, or $CD68^+$ monocytes/macrophages in *Il15*Δ/Δ rats, it is possible that IL15 deficiency in rats may impact the development or survival of specific subsets of these cells, or affect other immune or nonimmune cells. Likewise, it cannot be confirmed whether *Il15*Δ/Δ rats possess defects in all subsets of NK cells. A more thorough characterization of different subtypes of NK cells in rats is needed before this can be determined.

The significance of uterine NK cells has long mystified reproductive biologists. Natural killer cells in blood and many other tissues secrete cytokines and chemokines that influence immune responses, and also function in the recognition and elimination of both cancerous and virally infected cells [30, 31]. It is tempting to speculate that uterine NK cells would have a similar function. However, uterine NK cells are phenotypically and functionally different than other tissue-resident NK cells [32–34]. For example, uterine NK cells possess a distinct cell surface receptor repertoire compared to peripheral blood NK cells, produce an abundant array of cytokines and angiogenic growth factors, and, despite possessing prominent granules containing proteins such as granzyme, perforin, and granulysin, are only weakly cytotoxic [35]. This suggests that uterine NK cells likely possess other, nonimmunological functions. To date, the most established functions of uterine NK cells were discovered by studies using NK-cell-deficient mice [36]. Mice have been rendered NK-cell deficient or nonfunctional by (i) expression of the tgε26 transgene [37], (ii) through *Il15* deficiency [22], (iii) by null mutations in the genes encoding common cytokine receptor gamma chain (which includes a component of the IL15 receptor) and recombination activating gene 2 [38], (iv) by transgenic expression of Ly49A [39], and (v) by knocking out the basic leucine zipper transcription factor E4BP4 (which acts downstream of the IL15 receptor) [40]. The impact of NK-cell deficiency on uterine vascular development and pregnancy outcome has been described in the first three models. All three models display deficiencies in pregnancy-dependent changes to the uterine vasculature, including relatively thick-walled spiral arteries with narrow lumens compared to wild-type mice. These observations have shaped the notion that NK cells initiate development of the uterine vasculature that, in turn, optimizes blood flow to the developing placenta [36]. Ex vivo studies using decidual NK cells isolated from human pregnancies have shown a similar vascular destabilizing function of these cells, suggesting that NK-cell actions on the uterine vasculature is a conserved feature among multiple species [41].

Despite the role of uterine NK cells in early spiral artery development, pregnancy proceeds without any obvious deficit in fetal viability in mice lacking NK cells. This is consistent with what we observed in the current study using NK-cell-deficient rats, where no changes in litter size or resorption rate were evident in NK-cell-deficient rats compared with wild-type rats. Thus, at least in mice and rats, uterine NK cells do not appear to be compulsory for any activities encompassing a viable pregnancy (implantation, placentation, or parturition), nor are they essential for fetal development and survival [42]. One admonition of our findings in NK-cell-deficient rats and observations reported using NK-cell-deficient mice is the relative cleanliness of the environment in which they are housed. Consequently, the immune status of laboratory animals is in an immature state relative to wild animals [43]. Comparisons between

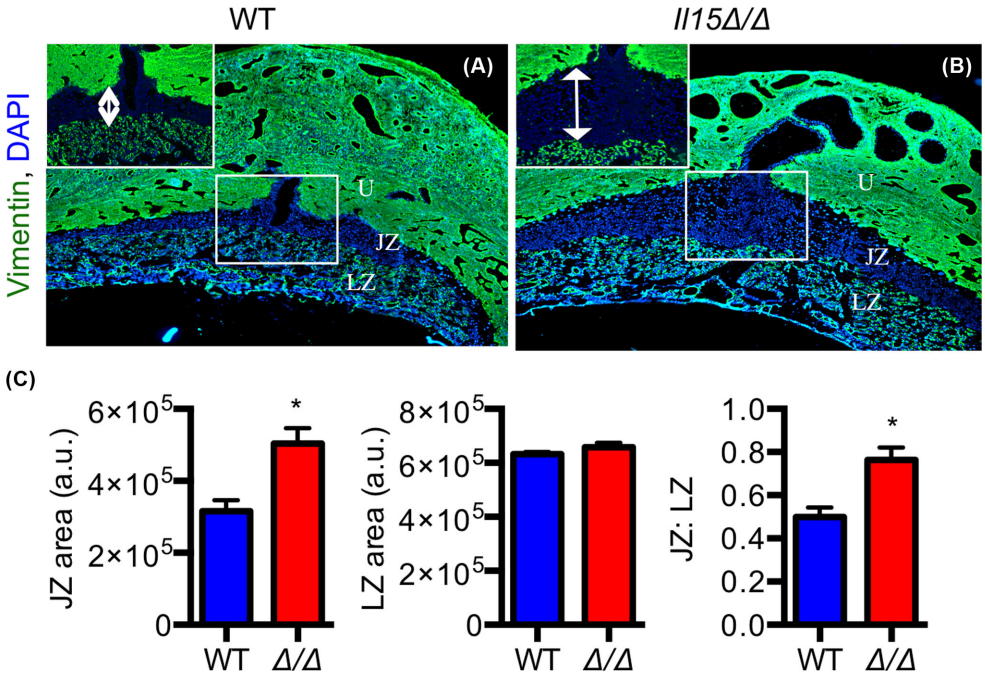

Figure 6. Enhanced junctional zone size in *Il15*Δ/Δ rats. Placentation sites from E13.5 wild-type (WT; **A**) and *Il15*Δ/Δ (**B**) rats were examined using immunohistochemistry for vimentin, which demarcates the zones of the placenta (labyrinth zone, LZ; junctional zone, JZ; and uterus, U). Note the expanded JZ (the placental zone where invasive trophoblast cells originate). A magnified view of the JZ is shown in the boxed insets. The sizes of the LZ and JZ, and a size ratio between the two zones, are graphically depicted in (**C**). Graphs represent means +/− SEM. Asterisks denote statistical significance (*, $P < 0.05$, n = 5).

wild-type and NK-cell-deficient animals living in the wild may reveal additional functions of uterine NK cells during pregnancy. Another possible explanation for the lack of apparent effect on pregnancy outcome is that the absence of NK cells in the uterus may be compensated by the presence of other innate lymphoid cells that are not dependent on IL15 for their expansion and survival, but which can exert similar functions as NK cells [44]. It is interesting to note that changes in the number or activity of uterine NK cells have been associated with various pregnancy complications in humans such as fetal growth restriction, preeclampsia, and recurrent spontaneous abortion [15, 45–51]. Therefore, although uterine NK cells do not appear to be essential for progression of normal pregnancy, they may have important regulatory roles that can affect maternal health and fetal growth.

In line with the functions of uterine NK cells in the early stages of spiral artery development, it has been hypothesized that NK cells are a precondition for proper trophoblast invasion and trophoblast-directed spiral artery remodeling. For example, experiments performed in vitro using human cell models show that chemokines and growth factors produced by uterine NK cells enhance trophoblast invasion and trophoblast capillary network formation [33, 52–55]. However, in other reports the opposite action was reported: factors produced by uterine NK cells inhibit trophoblast invasion [56–59]. Discrepancies in results obtained in these studies may relate to the gestational age at which uterine NK cells were isolated, difficulty in obtaining healthy material from early gestation, and other procedural limitations of in vitro experimentation [53]. Determination of how NK cells influence trophoblast invasion in vivo is warranted. In the current study using rats, we found that NK cells are not a prerequisite for robust endovascular trophoblast invasion. Rather, accelerated and more profound trophoblast invasion into spiral arteries was observed in rats devoid of NK cells. This is consistent with findings using NK-cell-immunodepleted rats [16]. In addition to extensive trophoblast invasion into spiral arteries, NK-cell-deficient rats exhibit extensive loss of vascular smooth muscle surrounding the spiral arteries at midgestation, concomitant with enhanced dilation of these vessels compared to wild-type rats. Thus, NK cells are not required for trophoblast-mediated removal of spiral artery endothelium and destruction of the vascular media. Rather, NK cells appear to have a restraining effect on trophoblast incursion into the spiral arteries, temporarily delaying trophoblast-directed vascular remodeling. This finding is logical, given that the onset of trophoblast invasion generally coincides with decline of uterine NK cells [6, 60, 61].

Two plausible interpretations can be extrapolated from our findings that rats lacking NK cells exhibit accelerated trophoblast invasion. The first explanation is that uterine NK cells effectively delay and delimit trophoblast invasion, thereby protecting the mother from overly aggressive trophoblast invasion. In support of this interpretation, decreased NK-cell number has been associated with an increased predisposition to develop serious hyperinvasive trophoblastic disorders such as placenta accreta [62, 63]. Invasive trophoblast cells extending too deep into the uterus can complicate parturition and pose a serious health risk for the mother. Thus, uterine NK cells in this context may be viewed as a maternal protective strategy to control the depth of trophoblast invasion. Intriguingly, the depth of trophoblast invasion at later time points in gestation was equivalent between wild-type and NK-cell-deficient rats, and no NK-cell-deficient rats died during parturition.

The second interpretation is that accelerated trophoblast invasion is an adaptive strategy mediated by the placenta in response

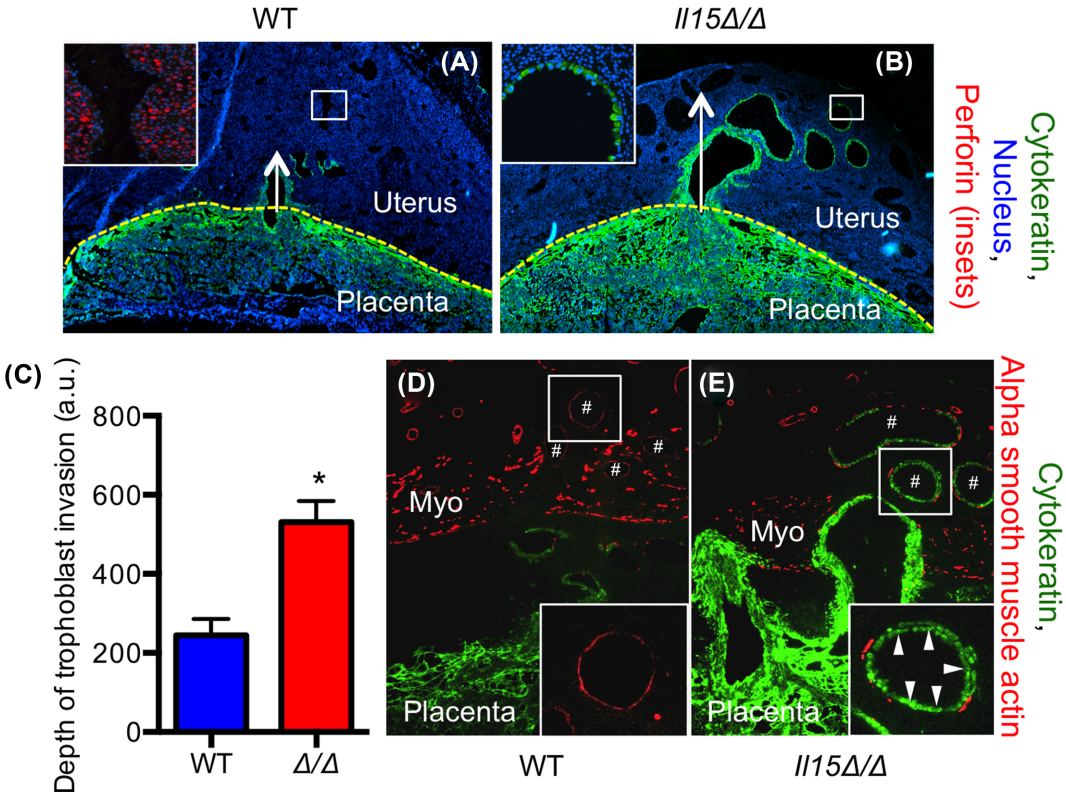

Figure 7. Accelerated trophoblast invasion in NK-cell-deficient rats. Trophoblast cells from E13.5 wild-type (WT; **A**) and *Il15*Δ/Δ (**B**) rats were immunostained using cytokeratin. The yellow dashed line demarcates the boundary between placenta and uterus. Note the increased depth of trophoblast invasion into the uterus, and increased numbers of dilated spiral arteries in *Il15*Δ/Δ rats. Magnified views of spiral arteries are shown in the upper left corners. In these insets, perforin immunostaining (for NK cells) is also shown. Note the absence of NK cells and presence of trophoblast cells within the spiral arteries in (**B**). Depth of trophoblast invasion is graphically depicted in (**C**). Immunostaining for alpha smooth muscle actin (red, showing both uterine myometrial smooth muscle (Myo) in bright red and vascular smooth muscle surrounding the vessels) is shown within the uterine mesometrial compartment in WT (**D**) and *Il15*Δ/Δ (**E**) dams. Trophoblast cells situated within the spiral arteries are stained using cytokeratin (green). Spiral arteries are labeled with a number sign (#). A boxed inset of representative spiral arteries from WT (containing no trophoblast cells) and *Il15*Δ/Δ rats is shown in the lower left corner. Note that the smooth muscle layer is absent in portions of spiral arteries containing trophoblast cells (arrowheads). Graphs represent means +/− SEM. Asterisks denote statistical significance (*, $P < 0.05$, n = 4).

to a lack of NK-cell-directed uterine vascular development early in pregnancy. In support of this interpretation, the placenta is a dynamic organ that can adjust its capacity to supply nutrients and oxygen in response to intrinsic or extrinsic changes in the maternal or fetal environment. Adaptations may include structural alterations (e.g., changes in the volume or composition of the junctional and labyrinth zones) and functional modifications (e.g.., activation of genes that alter the operational capacity of the placenta). The ability of the placenta to adjust to changes in the intrauterine environment is dependent on the nature of the stress and the time and duration in which the stress appears. Such triggers may include hypoxia, maternal undernutrition, underlying maternal metabolic or immune pathologies, hormonal imbalances, or dysregulation of genes implicated in fetal or placental growth [64]. Previously, we observed that immunodepletion of NK cells in rats caused localized decidual hypoxia proximate to the developing placenta [16]. This was an expected outcome given the known importance of uterine NK cells for initiating decidual spiral artery development during pregnancy. In that study and the current study, we noted that maternal NK-cell deficiency was associated with expansion of the junctional zone, concomitant with accelerated invasion of trophoblast cells, and enhanced trophoblast-mediated spiral artery remodeling. Interestingly, this same phenotype is evident when pregnant rats are placed in low oxygen atmospheres early in pregnancy [65, 66]. Furthermore, rat trophoblast stem cells exposed to a hypoxic environment in vitro preferentially differentiate toward a junctional zone/invasive trophoblast lineage [16, 66]. Thus, the placenta exhibits a great deal of plasticity to sense low oxygen levels early in pregnancy (either due to a lack of NK-cell-mediated vascular development or systemic deficiency in oxygen delivery), and to respond accordingly to ensure that appropriate oxygen reaches the placenta prior to the onset of robust fetal growth. Placental adaptations to the loss of NK cells may at least partially explain why no significant fetal growth restriction or death was evident in our model. Defective coping mechanisms by the placenta in response to changes in the intrauterine environment may underlie some obstetric complications linked with trophoblast hyperinvasion (placenta accreta/percreta/increta) or hypoinvasion (preeclampsia and intrauterine growth restriction).

In conclusion, we have successfully generated an *Il15*-deficient rat model that exhibits impaired NK-cell development. NK-cell deficiency during pregnancy caused dramatic alterations to placental structure. Future studies should be aimed at deciphering long-term consequences of these placental adaptations on the offspring.

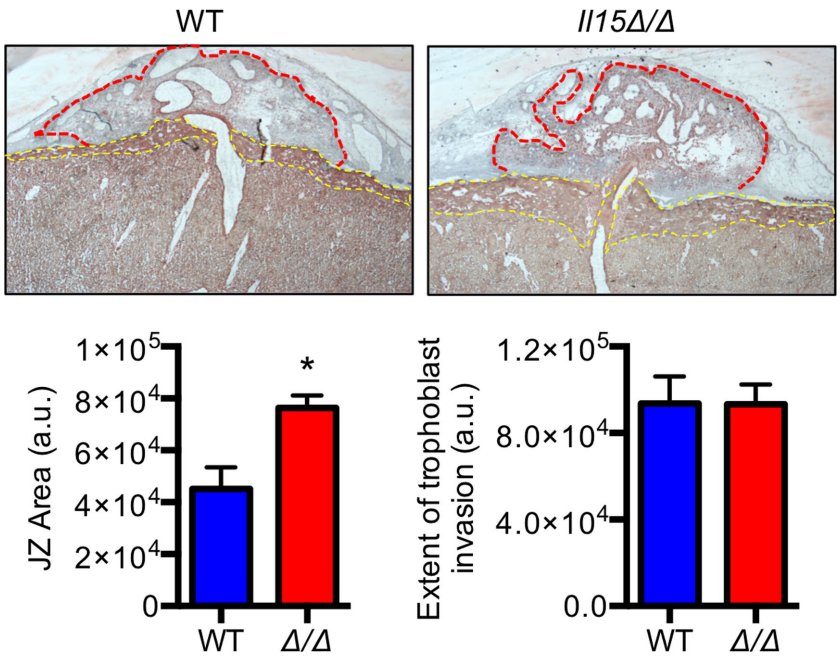

Figure 8. Extent of trophoblast invasion between wild-type and *Il15*Δ/Δ rats in later gestation. Trophoblast cells from E19.5 wild-type (WT) and *Il15*Δ/Δ were immunostained using cytokeratin. The perimeter of the junctional zone (JZ) is highlighted using a yellow dashed line; the area of the uterus in which trophoblast cells have invaded is outlined using a red dashed line. The area of the JZ is graphically depicted on the right. Graphs represent means +/− SEM. Asterisks denote statistical significance (*, $P < 0.05$, n = 3).

Supplementary data

Supplementary data are available at *BIOLRE* online.

Supplementary Figure S1. Determination of CD3 expression on the surface of KLRB1A^{hi} cells isolated from blood and spleen. (**A**) Representative images of CD3 in KLRB1A^{hi} cells isolated from blood (top panels) and spleen (bottom panels) from wild-type (WT) and *Il15*Δ/Δ rats. The x-axis represents forward scatter (FSC). (**B**) The percentage of KLRB1A^{hi} cells in blood and spleen from WT rats that express CD3 is graphically shown. Graphs represent means +/− SEM. Asterisks denote statistical significance (*$P < 0.05$, n = 3).

Supplementary Figure S2. Histological examination of placentation sites from wild-type and *Il15*Δ/Δ rats. Hematoxylin and eosin staining was conducted on sections taken from E13.5 wild-type (WT) and *Il15*Δ/Δ placentation sites. The left panels show representative low magnification images, whereas the right panels show high magnification images of the mesometrial compartment (Meso). Boxes in the left panels show the location of higher magnification images. Scale bar = 200 μm.

Acknowledgments

We thank Dr. Melissa Larson in the University of Kansas Medical Center Transgenic and Gene Targeting Institutional Facility, Dr. Pramod Dhakal for the PCR-based protocol used to determine rat fetal sex, and Stacy McClure for administrative assistance.

Conflict of Interest: The authors have declared that no conflict of interest exists.

References

1. Pijnenborg R, Vercruysse L, Hanssens M. The uterine spiral arteries in human pregnancy: facts and controversies. *Placenta* 2006; **27**:939–958.
2. Soares MJ, Chakraborty D, Kubota K, Renaud SJ, Rumi MA. Adaptive mechanisms controlling uterine spiral artery remodeling during the establishment of pregnancy. *Int J Dev Biol* 2014; **58**:247–259.
3. Malassine A, Frendo JL, Evain-Brion D. A comparison of placental development and endocrine functions between the human and mouse model. *Hum Reprod Update* 2003; **9**:531–539.
4. Kam EP, Gardner L, Loke YW, King A. The role of trophoblast in the physiological change in decidual spiral arteries. *Hum Reprod* 1999; **14**:2131–2138.
5. Carter AM, Enders AC. Comparative aspects of trophoblast development and placentation. *Reprod Biol Endocrinol* 2004; **2**:46.
6. Ain R, Canham LN, Soares MJ. Gestation stage-dependent intrauterine trophoblast cell invasion in the rat and mouse: novel endocrine phenotype and regulation. *Dev Biol* 2003; **260**:176–190.
7. Caluwaerts S, Vercruysse L, Luyten C, Pijnenborg R. Endovascular trophoblast invasion and associated structural changes in uterine spiral arteries of the pregnant rat. *Placenta* 2005; **26**:574–584.
8. Brosens I, Pijnenborg R, Vercruysse L, Romero R. The "Great Obstetrical Syndromes" are associated with disorders of deep placentation. *Am J Obstet Gynecol* 2011; **204**:193–201.
9. King A, Balendran N, Wooding P, Carter NP, Loke YW. CD3- leukocytes present in the human uterus during early placentation: phenotypic and morphologic characterization of the CD56++ population. *Dev Immunol* 1991; **1**:169–190.
10. Bulmer JN, Williams PJ, Lash GE. Immune cells in the placental bed. *Int J Dev Biol* 2010; **54**:281–294.
11. Moffett A, Colucci F. Uterine NK cells: active regulators at the maternal-fetal interface. *J Clin Invest* 2014; **124**:1872–1879.
12. Hofmann AP, Gerber SA, Croy BA. Uterine natural killer cells pace early development of mouse decidua basalis. *Mol Hum Reprod* 2014; **20**:66–76.
13. Barber EM, Pollard JW. The uterine NK cell population requires IL-15 but these cells are not required for pregnancy nor the resolution of a Listeria monocytogenes infection. *J Immunol* 2003; **171**:37–46.
14. Ashkar AA, Black GP, Wei Q, He H, Liang L, Head JR, Croy BA. Assessment of requirements for IL-15 and IFN regulatory factors in uterine

NK cell differentiation and function during pregnancy. *J Immunol* 2003; **171**:2937–2944.
15. Kieckbusch J, Gaynor LM, Moffett A, Colucci F. MHC-dependent inhibition of uterine NK cells impedes fetal growth and decidual vascular remodelling. *Nat Commun* 2014; **5**:3359.
16. Chakraborty D, Rumi MA, Konno T, Soares MJ. Natural killer cells direct hemochorial placentation by regulating hypoxia-inducible factor dependent trophoblast lineage decisions. *Proc Natl Acad Sci USA* 2011; **108**:16295–16300.
17. Smith SD, Dunk CE, Aplin JD, Harris LK, Jones RL. Evidence for immune cell involvement in decidual spiral arteriole remodeling in early human pregnancy. *Am J Pathol* 2009; **174**:1959–1971.
18. Fehniger TA, Caligiuri MA. Interleukin 15: biology and relevance to human disease. *Blood* 2001; **97**:14–32.
19. Urnov FD, Rebar EJ, Holmes MC, Zhang HS, Gregory PD. Genome editing with engineered zinc finger nucleases. *Nat Rev Genet* 2010; **11**:636–646.
20. Clapcote SJ, Roder JC. Simplex PCR assay for sex determination in mice. *Biotechniques* 2005; **38**:702, 704, 706.
21. Schneider CA, Rasband WS, Eliceiri KW. NIH Image to ImageJ: 25 years of image analysis. *Nat Methods* 2012; **9**:671–675.
22. Kennedy MK, Glaccum M, Brown SN, Butz EA, Viney JL, Embers M, Matsuki N, Charrier K, Sedger L, Willis CR, Brasel K, Morrissey PJ et al. Reversible defects in natural killer and memory CD8 T cell lineages in interleukin 15-deficient mice. *J Exp Med* 2000; **191**:771–780.
23. Pistilli EE, Bogdanovich S, Garton F, Yang N, Gulbin JP, Conner JD, Anderson BG, Quinn LS, North K, Ahima RS, Khurana TS. Loss of IL-15 receptor alpha alters the endurance, fatigability, and metabolic characteristics of mouse fast skeletal muscles. *J Clin Invest* 2011; **121**:3120–3132.
24. Bustamante JJ, Dai G, Soares MJ. Pregnancy and lactation modulate maternal splenic growth and development of the erythroid lineage in the rat and mouse. *Reprod Fertil Dev* 2008; **20**:303–310.
25. Georgiades P, Ferguson-Smith AC, Burton GJ. Comparative developmental anatomy of the murine and human definitive placentae. *Placenta* 2002; **23**:3–19.
26. Chae DW, Nosaka Y, Strom TB, Maslinski W. Distribution of IL-15 receptor alpha-chains on human peripheral blood mononuclear cells and effect of immunosuppressive drugs on receptor expression. *J Immunol* 1996; **157**:2813–2819.
27. Suzuki H, Duncan GS, Takimoto H, Mak TW. Abnormal development of intestinal intraepithelial lymphocytes and peripheral natural killer cells in mice lacking the IL-2 receptor beta chain. *J Exp Med* 1997; **185**: 499–505.
28. Imada K, Bloom ET, Nakajima H, Horvath-Arcidiacono JA, Udy GB, Davey HW, Leonard WJ. Stat5b is essential for natural killer cell-mediated proliferation and cytolytic activity. *J Exp Med* 1998; **188**: 2067–2074.
29. Ye W, Zheng LM, Young JD, Liu CC. The involvement of interleukin (IL)-15 in regulating the differentiation of granulated metrial gland cells in mouse pregnant uterus. *J Exp Med* 1996; **184**:2405–2410.
30. Morvan MG, Lanier LL. NK cells and cancer: you can teach innate cells new tricks. *Nat Rev Cancer* 2016; **16**:7–19.
31. Yokoyama WM, Kim S, French AR. The dynamic life of natural killer cells. *Annu Rev Immunol* 2004; **22**:405–429.
32. Koopman LA, Kopcow HD, Rybalov B, Boyson JE, Orange JS, Schatz F, Masch R, Lockwood CJ, Schachter AD, Park PJ, Strominger JL. Human decidual natural killer cells are a unique NK cell subset with immunomodulatory potential. *J Exp Med* 2003; **198**:1201–1212.
33. Hanna J, Goldman-Wohl D, Hamani Y, Avraham I, Greenfield C, Natanson-Yaron S, Prus D, Cohen-Daniel L, Arnon TI, Manaster I, Gazit R, Yutkin V et al. Decidual NK cells regulate key developmental processes at the human fetal-maternal interface. *Nat Med* 2006; **12**: 1065–1074.
34. Sojka DK, Plougastel-Douglas B, Yang L, Pak-Wittel MA, Artyomov MN, Ivanova Y, Zhong C, Chase JM, Rothman PB, Yu J, Riley JK, Zhu J et al. Tissue-resident natural killer (NK) cells are cell lineages distinct from thymic and conventional splenic NK cells. *Elife* 2014; **3**:e01659.
35. Ferry BL, Starkey PM, Sargent IL, Watt GM, Jackson M, Redman CW. Cell populations in the human early pregnancy decidua: natural killer activity and response to interleukin-2 of CD56-positive large granular lymphocytes. *Immunology* 1990; **70**:446–452.
36. Croy BA, He H, Esadeg S, Wei Q, McCartney D, Zhang J, Borzychowski A, Ashkar AA, Black GP, Evans SS, Chantakru S, van den Heuvel M et al. Uterine natural killer cells: insights into their cellular and molecular biology from mouse modelling. *Reproduction* 2003; **126**: 149–160.
37. Wang B, Biron C, She J, Higgins K, Sunshine MJ, Lacy E, Lonberg N, Terhorst C. A block in both early T lymphocyte and natural killer cell development in transgenic mice with high-copy numbers of the human CD3E gene. *Proc Natl Acad Sci USA* 1994; **91**:9402–9406.
38. Mazurier F, Fontanellas A, Salesse S, Taine L, Landriau S, Moreau-Gaudry F, Reiffers J, Peault B, Di Santo JP, de Verneuil H. A novel immunodeficient mouse model–RAG2 x common cytokine receptor gamma chain double mutants–requiring exogenous cytokine administration for human hematopoietic stem cell engraftment. *J Interferon Cytokine Res* 1999; **19**:533–541.
39. Kim S, Iizuka K, Aguila HL, Weissman IL, Yokoyama WM. In vivo natural killer cell activities revealed by natural killer cell-deficient mice. *Proc Natl Acad Sci USA* 2000; **97**:2731–2736.
40. Gascoyne DM, Long E, Veiga-Fernandes H, de Boer J, Williams O, Seddon B, Coles M, Kioussis D, Brady HJ. The basic leucine zipper transcription factor E4BP4 is essential for natural killer cell development. *Nat Immunol* 2009; **10**:1118–1124.
41. Robson A, Harris LK, Innes BA, Lash GE, Aljunaidy MM, Aplin JD, Baker PN, Robson SC, Bulmer JN. Uterine natural killer cells initiate spiral artery remodeling in human pregnancy. *FASEB J* 2012; **26**: 4876–4885.
42. Bany BM, Scott CA, Eckstrum KS. Analysis of uterine gene expression in interleukin-15 knockout mice reveals uterine natural killer cells do not play a major role in decidualization and associated angiogenesis. *Reproduction* 2012; **143**:359–375.
43. Beura LK, Hamilton SE, Bi K, Schenkel JM, Odumade OA, Casey KA, Thompson EA, Fraser KA, Rosato PC, Filali-Mouhim A, Sekaly RP, Jenkins MK et al. Normalizing the environment recapitulates adult human immune traits in laboratory mice. *Nature* 2016; **532**:512–516.
44. Doisne JM, Balmas E, Boulenouar S, Gaynor LM, Kieckbusch J, Gardner L, Hawkes DA, Barbara CF, Sharkey AM, Brady HJ, Brosens JJ, Moffett A et al. Composition, Development, and Function of Uterine Innate Lymphoid Cells. *J Immunol* 2015; **195**:3937–3945.
45. Wallace AE, Host AJ, Whitley GS, Cartwright JE. Decidual natural killer cell interactions with trophoblasts are impaired in pregnancies at increased risk of preeclampsia. *Am J Pathol* 2013; **183**:1853–1861.
46. Wallace AE, Fraser R, Gurung S, Goulwara SS, Whitley GS, Johnstone AP, Cartwright JE. Increased angiogenic factor secretion by decidual natural killer cells from pregnancies with high uterine artery resistance alters trophoblast function. *Hum Reprod* 2014; **29**:652–660.
47. Hiby SE, Apps R, Sharkey AM, Farrell LE, Gardner L, Mulder A, Claas FH, Walker JJ, Redman CW, Morgan L, Tower C, Regan L et al. Maternal activating KIRs protect against human reproductive failure mediated by fetal HLA-C2. *J Clin Invest* 2010; **120**:4102–4110.
48. Moffett A, Regan L, Braude P. Natural killer cells, miscarriage, and infertility. *BMJ* 2004; **329**:1283–1285.
49. Hiby SE, Walker JJ, O'Shaughnessy K M, Redman CW, Carrington M, Trowsdale J, Moffett A. Combinations of maternal KIR and fetal HLA-C genes influence the risk of preeclampsia and reproductive success. *J Exp Med* 2004; **200**:957–965.
50. Sharma S. Natural killer cells and regulatory T cells in early pregnancy loss. *Int J Dev Biol* 2014; **58**:219–229.
51. Murphy SP, Hanna NN, Fast LD, Shaw SK, Berg G, Padbury JF, Romero R, Sharma S. Evidence for participation of uterine natural killer cells in the mechanisms responsible for spontaneous preterm labor and delivery. *Am J Obstet Gynecol* 2009; **200**:308. e301–309.
52. Xiong S, Sharkey AM, Kennedy PR, Gardner L, Farrell LE, Chazara O, Bauer J, Hiby SE, Colucci F, Moffett A. Maternal uterine NK

cell-activating receptor KIR2DS1 enhances placentation. *J Clin Invest* 2013; **123**:4264–4272.
53. Lash GE, Otun HA, Innes BA, Percival K, Searle RF, Robson SC, Bulmer JN. Regulation of extravillous trophoblast invasion by uterine natural killer cells is dependent on gestational age. *Hum Reprod* 2010; **25**:1137–1145.
54. Hu Y, Eastabrook G, Tan R, MacCalman CD, Dutz JP, von Dadelszen P. Decidual NK cell-derived conditioned medium enhances capillary tube and network organization in an extravillous cytotrophoblast cell line. *Placenta* 2010; **31**:213–221.
55. Chauhan M, Balakrishnan M, Yallampalli U, Endsley J, Hankins GD, Theiler R, Yallampalli C. Adrenomedullin 2/intermedin regulates HLA-G in human trophoblasts. *Biol Reprod* 2011; **85**:1232–1239.
56. Hu Y, Dutz JP, MacCalman CD, Yong P, Tan R, von Dadelszen P. Decidual NK cells alter in vitro first trimester extravillous cytotrophoblast migration: a role for IFN-gamma. *J Immunol* 2006; **177**: 8522–8530.
57. Lash GE, Otun HA, Innes BA, Kirkley M, De Oliveira L, Searle RF, Robson SC, Bulmer JN. Interferon-gamma inhibits extravillous trophoblast cell invasion by a mechanism that involves both changes in apoptosis and protease levels. *FASEB J* 2006; **20**:2512–2518.
58. Bauer S, Pollheimer J, Hartmann J, Husslein P, Aplin JD, Knofler M. Tumor necrosis factor-alpha inhibits trophoblast migration through elevation of plasminogen activator inhibitor-1 in first-trimester villous explant cultures. *J Clin Endocrinol Metab* 2004; **89**:812–822.
59. Lash GE, Otun HA, Innes BA, Bulmer JN, Searle RF, Robson SC. Inhibition of trophoblast cell invasion by TGFB1, 2, and 3 is associated with a decrease in active proteases. *Biol Reprod* 2005; **73**:374–381.
60. Konno T, Rempel LA, Arroyo JA, Soares MJ. Pregnancy in the brown Norway rat: a model for investigating the genetics of placentation. *Biol Reprod* 2007; **76**:709–718.
61. Bulmer JN, Lash GE. Human uterine natural killer cells: a reappraisal. *Mol Immunol* 2005; **42**:511–521.
62. Laban M, Ibrahim EA, Elsafty MS, Hassanin AS. Placenta accreta is associated with decreased decidual natural killer (dNK) cells population: a comparative pilot study. *Eur J Obstet Gynecol Reprod Biol* 2014; **181**:284–288.
63. Tantbirojn P, Crum CP, Parast MM. Pathophysiology of placenta creta: the role of decidua and extravillous trophoblast. *Placenta* 2008; **29**: 639–645.
64. Sandovici I, Hoelle K, Angiolini E, Constancia M. Placental adaptations to the maternal-fetal environment: implications for fetal growth and developmental programming. *Reprod Biomed Online* 2012; **25**:68–89.
65. Rosario GX, Konno T, Soares MJ. Maternal hypoxia activates endovascular trophoblast cell invasion. *Dev Biol* 2008; **314**:362–375.
66. Chakraborty D, Cui W, Rosario GX, Scott RL, Dhakal P, Renaud SJ, Tachibana M, Rumi MA, Mason CW, Krieg AJ, Soares MJ. HIF-KDM3A-MMP12 regulatory circuit ensures trophoblast plasticity and placental adaptations to hypoxia. *Proc Natl Acad Sci USA* 2016; **113**:E7212–E7221.